

## Supplementary Information

### Lead-Free Double-Perovskite Cs<sub>4</sub>CuSb<sub>2</sub>Cl<sub>12</sub> as an Efficient Saturable Absorber for Q-Switched Mode-locking Fiber Lasers

Hui-Jie Zhang <sup>a,‡</sup>, Tao Song <sup>a,‡</sup>, Xin-Xing Liu <sup>b,‡</sup>, Ming-Zhu Chen <sup>a</sup>, Bo Ma <sup>a</sup>, Han-Zhi Huang <sup>a</sup>, Xin-Ping Zhai <sup>a</sup>, Qiang Wang <sup>a, \*</sup>, Yu-Long Tang <sup>b, \*</sup>, Hao-Li Zhang <sup>a, \*</sup>

<sup>a</sup> State Key Laboratory of Applied Organic Chemistry (SKLAOC), Key Laboratory of Nonferrous Metal Chemistry and Resources Utilization of Gansu Province, College of Chemistry and Chemical Engineering, Key Laboratory of Special Function Materials and Structure Design, Ministry of Education, Lanzhou University, Lanzhou, 730000, China.

<sup>b</sup> The key Laboratory for Laser Plasmas (MOE), School of Physics and Astronomy, Collaborative Innovation Center of IFSA, Shanghai Jiao Tong University, Shanghai 200240, China.

<sup>‡</sup> The authors equally contributed to the manuscript.

#### Correspondence authors:

qiangwang@lzu.edu.cn. (Q.W.);

yulong@sjtu.edu.cn. (Y.-L. T)

haoli.zhang@lzu.edu.cn. (H.-L. Z.);

## **Chemicals**

Cesium chloride (CsCl, 99.99%) and cuprous chloride (CuCl 99.99%) were purchased from Aladdin Chemistry Co. Ltd. Antimonous chloride (SbCl<sub>3</sub>, 99.9%) was purchased from Damas-beta (Shanghai) Chemistry Co. Ltd. Hydrochloric acid (HCl, 38% in water by weight) was purchased from Chengdu Kelong Chemical Reagent Co., Ltd. Dimethyl sulphoxide (DMSO) and *N, N*-Dimethylformamide (DMF) was from Aladdin Chemistry Co. Ltd. All solvents and chemicals were used without any further purification. Deionized water with a resistivity of 18.3 MΩ•cm was used to prepare an aqueous solution throughout the experiment.

## **Characterization methods**

### *Spectroscopic measurements*

The UV-vis-NIR absorption spectra were collected on a TU-1810 spectrophotometer (Beijing Purkinje General Instrument, China). The UV-vis diffuse reflectance spectra were collected using a Shimadzu UV Probe 2600 (pure BaSO<sub>4</sub> as the background). Femtosecond transient absorption (TA) experiments were conducted on Helios transient absorption spectrometer (Ultrafast Systems), employing the regenerative amplifier (<110 fs, 1 kHz, 800 nm) (Coherent Legend Elite) as laser source seeded by a Coherent Chameleon oscillator (75 fs, 80 MHz). The supercontinuum white probe pulses at the range of 330-600 nm, 425-800 nm, and 850-1600 nm were generated on CaF<sub>2</sub>, sapphire, and YAG crystals excited by the small portion 800-nm laser beam from the amplifier with appropriate beam intensity. The 350-nm pump pulses were generated from a Light Conversion OPerA-Solo optical parametric amplifier (285-2600

nm), and 400-nm pump pulses were generated from the main portion 800-nm laser beam through the SHG effect of the BBO crystal. To prevent the dipole-dipole interactions between the excited molecules and the probe light, the polarization of the pump and probe was set at the magic angle ( $54.7^\circ$ ) when 350-nm pump pulses as the pump beam. The data analysis was conducted using Surface Xplore software that comes with Helios (Ultrafast Systems, LLC).

#### *Z-scan measurements*

The Z-scan setup comprises a Q-switched Nd: YAG laser (Continuum, Model Surelite SL-I-10), optical elements and photodetectors. The laser has two output wavelengths of 532 nm and 1064 nm, with an FWHM of  $\sim 4$  ns and a repetition rate of 10 Hz. The temporal and spatial profiles of the output pulses were customized with an approximately Gaussian distribution. The radius of the optical spot at the focus point was about 30  $\mu\text{m}$ .

#### *I-scan measurements*

With the same Z-scan setup, but the sample is fixed at the focus position of the optical path of the apparatus. The normalized transmittance of the sample as a function of the input fluence (energy) is measured by using a 532 nm laser output. The detailed setup was described in our previous work.<sup>1,2</sup>

#### *Other characterizations*

Powder X-ray diffraction (XRD) patterns of the products were recorded on a Panalytical X'Pert PRO diffractometer using Cu K  $\alpha$  X-rays between  $5^\circ$  and  $90^\circ$ . The morphology of samples was obtained on field-emission scanning electron microscopy

(FE-SEM, Hitachi S4800) at an accelerating voltage of 5.0 kV. X-ray photoelectron spectroscopy (XPS) was performed on an AXIS Ultra. The thermogravimetric analysis (TGA) was performed on a Linseis PT 1600 in the temperature interval 25-850 °C at a ramping rate of 20 °C min<sup>-1</sup> under N<sub>2</sub> atmosphere.

#### *Q-Switched mode-locking experiment*

A clear solution was formed by dissolving 5mg Cs<sub>4</sub>CuSb<sub>2</sub>Cl<sub>12</sub> crystals in 1.5 mL dimethyl sulfoxide (DMSO), and the Cs<sub>4</sub>CuSb<sub>2</sub>Cl<sub>12</sub> saturable absorber (SA) was obtained by spin-coating onto a gold mirror and annealing at 110°C for 30 min. A ring cavity was adopted, which was comprised of a fiber combiner, a 5-m-long segment of Yb-doped double-clad fiber (10/125 μm core/clad, absorption of 4.95 dB/m @976 nm, Nufern Co.), a fiber circulator, a 20/80 fiber coupler (80% recoupled to the cavity) and the as-fabricated Cs<sub>4</sub>CuSb<sub>2</sub>Cl<sub>12</sub> SA. A 976 nm laser diode (Bwt-bj Co.) was used as the pump source. The pump light was coupled into the Yb-doped fiber through the fiber combiner. The fiber circulator ensures unidirectional light propagation in the ring cavity with a definite light propagation direction. The port-pigtail of the circulator was cleaved perpendicularly and positioned in close proximity to the Cs<sub>4</sub>CuSb<sub>2</sub>Cl<sub>12</sub>-SA for light modulation and feedback. A power meter (Thorlabs, PM320E), spectrometer (SIR5000, Ocean Optics) and real-time oscilloscope (500 MHz, Tektronix, TDS3052B) in combination with a photodetector (10 GHz, Newport) were used to measure the laser output power, spectra, and temporal pulses, respectively. The spectrum was recorded by an infrared spectrometer (AQ4037, YOKOGAWA) with a resolution of 0.1 nm.

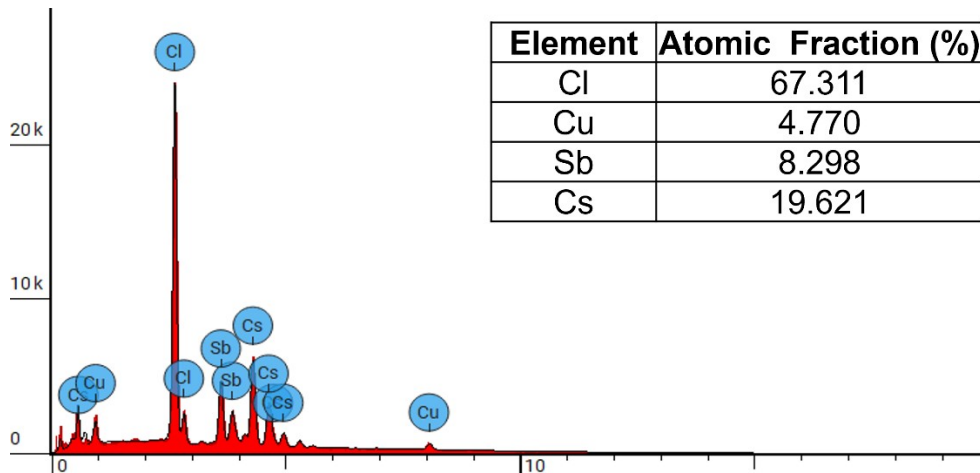


**Figure S1.** The EDS spectrum of the  $\text{Cs}_4\text{CuSb}_2\text{Cl}_{12}$  crystal.

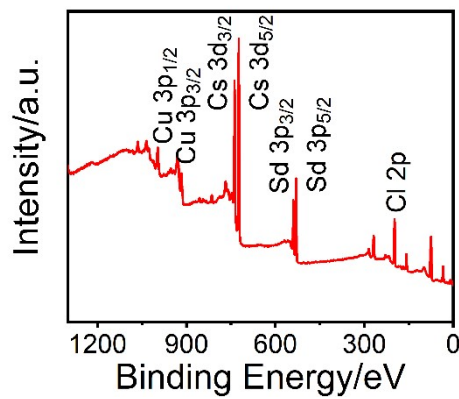


**Figure S2.** The XPS survey spectra of the  $\text{Cs}_4\text{CuSb}_2\text{Cl}_{12}$  crystal.



**Figure S3.** The schematic illustration of the preparation procedure of the  $\text{Cs}_4\text{CuSb}_2\text{Cl}_{12}$  thin film.

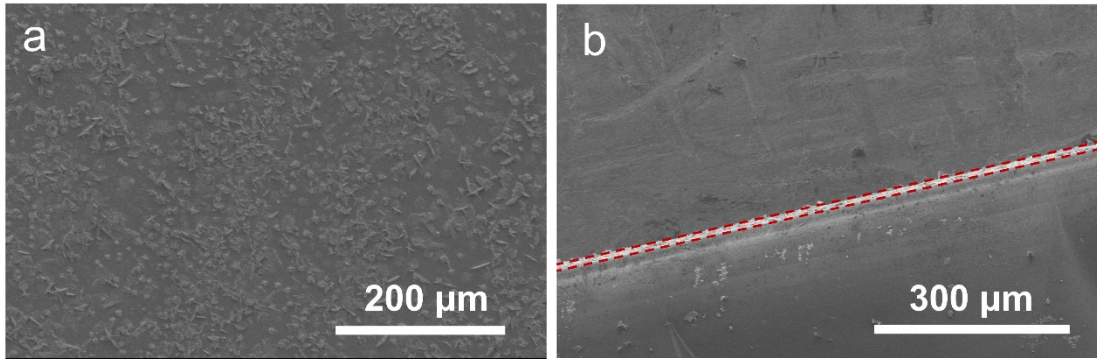


**Figure S4.** (a) The SEM image and (b) the cross-sectional SEM image of the  $\text{Cs}_4\text{CuSb}_2\text{Cl}_{12}$  thin film with different resolution. The thickness of pristine  $\text{Cs}_4\text{CuSb}_2\text{Cl}_{12}$  films is  $\sim 4 \mu\text{m}$ .

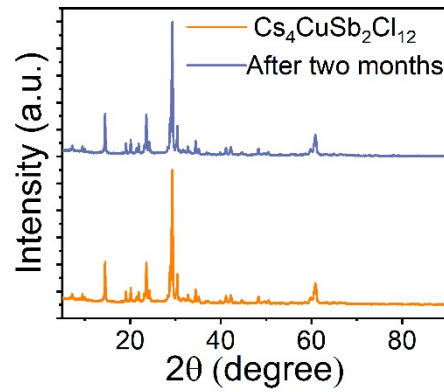


**Figure S5.** The XRD spectra of the  $\text{Cs}_4\text{CuSb}_2\text{Cl}_{12}$  thin film after two months.

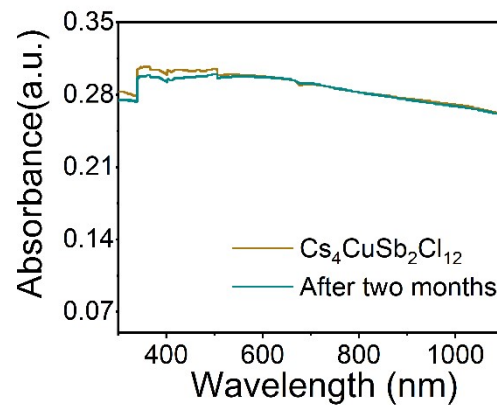


**Figure S6.** The absorbance evolution of the  $\text{Cs}_4\text{CuSb}_2\text{Cl}_{12}$  thin film over a long period of more than two months.

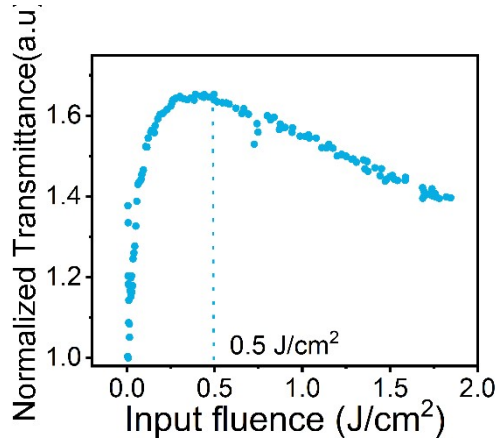


**Figure S7.** The normalized transmittance of the sample as a function of the input fluence measured by using a 532 nm laser output.

### The numerically fitting of Z-scan curves

The Z-scan data were fitted to the nonlinear transmission equation using a sum of two nonlinear absorptions with opposite signs:

$$\alpha(I) = \frac{\alpha_0}{1 + \frac{I}{I_s}} + \beta I$$

where  $\alpha(I)$  is the total nonlinear absorption coefficient,  $\alpha_0$  is the linear absorption coefficient,  $\beta$  is the negative nonlinear absorption coefficient,  $I$  is the incident laser intensity, and  $I_s$  is the saturation intensity, which is defined as the laser intensity at which  $\alpha_0$  drops to 50% of its initial value.

**Table S1** The summary of the fitted nonlinear optical parameters for the Cs<sub>4</sub>CuSb<sub>2</sub>Cl<sub>12</sub> thin film.

Samples	$\lambda_{\text{laser}}$ (nm)	E ( $\mu\text{J}$ )	T	$\beta$ (m/W)	Is (W/m <sup>2</sup> )
Cs <sub>4</sub> CuSb <sub>2</sub> Cl <sub>12</sub>	532	0.7	0.63	$-1.8 \times 10^{-7}$	$21.0 \times 10^{10}$
	532	0.9	0.63	$-1.7 \times 10^{-7}$	$9.0 \times 10^{10}$
	532	1.2	0.63	$-1.6 \times 10^{-7}$	$8.9 \times 10^{10}$
	532	1.4	0.63	$-1.4 \times 10^{-7}$	$9.2 \times 10^{10}$
	532	1.8	0.63	$-1.2 \times 10^{-7}$	$9.6 \times 10^{10}$
	1064	0.5	0.51	$-6.8 \times 10^{-7}$	$4.3 \times 10^{10}$
	1064	1.4	0.51	$-2.1 \times 10^{-7}$	$9.0 \times 10^{10}$

**Table S2** A comparison of nonlinear absorption coefficients of the Cs<sub>4</sub>CuSb<sub>2</sub>Cl<sub>12</sub> thin film with that of other materials

Sample	Wavelength (nm)	$\beta$ (m/W)	Is(W/cm <sup>2</sup> )	References
MAPbI <sub>3</sub> /ZnP2	515	$-2.4 \times 10^{-9}$	$1.27 \times 10^{10}$	3
Cs <sub>2</sub> AgBiBr <sub>6</sub> (D)	800	$-7.1 \times 10^{-8}$	NA	4
Au-CsPbBr <sub>3</sub>	800	$-2.3 \times 10^{-8}$	NA	5
MAPbI <sub>3</sub>	1028	$-5.0 \times 10^{-7}$	NA	6
CsPbBr <sub>3</sub>	1060	$-6.7 \times 10^{-13}$	NA	7
CH <sub>3</sub> NH <sub>3</sub> PbI <sub>3</sub>	1064	$-2.3 \times 10^{-8}$	NA	8
(C <sub>4</sub> H <sub>9</sub> NH <sub>3</sub> ) <sub>2</sub> (C H <sub>3</sub> NH <sub>2</sub> )Pb <sub>2</sub> I <sub>7</sub>	570	$-4.5 \times 10^{-7}$	$2.1 \times 10^{12}$	9
CsPbBr <sub>3</sub> QD	515	$-3.5 \times 10^{-12}$	$1.1 \times 10^{10}$	10
Bi	1064	$-3.9 \times 10^{-10}$	NA	11
Cs <sub>4</sub> CuSb <sub>2</sub> Cl <sub>12</sub>	532	$-1.8 \times 10^{-7}$	$9.6 \times 10^{10}$	<b>This work</b>
Cs <sub>4</sub> CuSb <sub>2</sub> Cl <sub>12</sub>	1064	$-6.8 \times 10^{-7}$	$9.0 \times 10^{10}$	<b>This work</b>

**Table S3** The extracted TA lifetime components of the Cs<sub>4</sub>CuSb<sub>2</sub>Cl<sub>12</sub> crystal.

Sample	Wavelength	$\tau_1$ (A1)	$\tau_2$ (A2)	$\tau_3$ (A3)
Cs <sub>4</sub> CuSb <sub>2</sub> Cl <sub>12</sub>	474	931 fs (39.0%)	283 ps (26.5%)	> ns (34.5%)
	605	822 fs (54.1%)	54.0 ps (27.5%)	> ns (18.4%)

**Table S4** Performance comparison of the Yb-doped fiber laser with different SAs.

SA	Wavelength	Pulse duration	Pump power	Output power	Laser efficiency	References
Ag/Mxene	1029.9 nm	4.9 $\mu$ s	65 mW	1.6 mW	NA	12
GaAs	1029.5 nm	4 ns	21.0 W	500 mW	6.3%	13
Ag nanoplates	1033.3 nm	1.01 $\mu$ s	600 mW	10.77 mW	2.7%	14
BP	1060.1 nm	4.21 $\mu$ s	400 mW	9.95 mW	12.43%	15
Bi <sub>2</sub> Te <sub>3</sub>	1046.2 nm	370 ns	5.4 W	57 mW	3.8%	16
Cu <sub>1.8</sub> S NCs	1567.2 nm	2 $\mu$ s	5.6 W	61.1 mW	1.0%	17
BiOCl	1046.7 nm	171.2 ns	28.0 W	1.8 W	10.9%	18
Cs <sub>x</sub> WO <sub>3</sub>	1030.0 nm	20.5 ns	160 mW	6.6 mW	5.0%	19
GaS	1066.9 nm	10 $\mu$ s	950 mW	13.72 mW	1.8%	20
Cs <sub>4</sub> CuSb <sub>2</sub> Cl <sub>12</sub>	1077.7 nm	2.1 $\mu$ s	1.8 W	112 mW	10.7%	<b>This work</b>

## References

1. S. Y. Wang, X. J. Zhen, Z. Z. Feng, M. J. Xiao, S. J. Li, W. Shang, Y. F. Huang, Q. Wang and H. L. Zhang, *J. Mater. Chem. C.*, 2022, **10**, 18025-18032.
2. X. P. Zhai, B. Ma, M. J. Xiao, W. Shang, Z. C. Zeng, Q. Wang and H. L. Zhang, *Nanoscale.*, 2023, **15**, 10606-10613.
3. Z. Guan, H. Li, Z. Wei, N. Shan, Y. Fang, Y. Zhao, L. Fu, Z. Huang, M. G. Humphrey and C. Zhang, *J. Mater. Chem. C.*, 2023, **11**, 1509-1521.
4. B. Li, H. Li, Y. Sun, M. G. Humphrey, C. Zhang and Z. Huang, *ACS Appl. Mater. Interfaces.*, 2023, **15**, 10858-10867.
5. X. Yan, Y. Shen, H. Liu and X. Yang, *J. Mater. Sci.*, 2020, **55**, 10678-10688.
6. B. S. Kalanoor, L. Gouda, R. Gottesman, S. Tirosh, E. Haltzi, A. Zaban and Y. R. Tischler, *ACS Photonics*, 2016, **3**, 361-370.
7. Z. Xu, T. Chen, D. Zhang, G. Zheng, J. Wu, J. Yan, X. Liu and J. Qiu, *J. Eur. Ceram. Soc.*, 2021, **41**, 729-734.
8. R. Zhang, J. Fan, X. Zhang, H. Yu, H. Zhang, Y. Mai, T. Xu, J. Wang and H. J. Snaith, *ACS Photonics*, 2016, **3**, 371-377.
9. I. Abdelwahab, P. Dichtl, G. Grinblat, K. Leng, X. Chi, I. H. Park, M. P. Nielsen, R. F. Oulton, K. P. Loh and S. A. Maier, *Adv. Mater.*, 2019, **31**, 1902685.
10. J. Li, H. Dong, B. Xu, S. Zhang, Z. Cai, J. Wang and L. Zhang, *Photonics Res.*, 2017, **5**, 457.
11. Q. Q. Yang, R. T. Liu, C. Huang, Y. F. Huang, L. F. Gao, B. Sun, Z. P. Huang, L. Zhang, C. X. Hu, Z. Q. Zhang, C. L. Sun, Q. Wang, Y. L. Tang and H. L. Zhang, *Nanoscale.*, 2018, **10**, 21106-21115.
12. J. Sun, H. Cheng, L. Xu, B. Fu, X. Liu and H. Zhang, *ACS Photonics*, 2023, **10**, 3133-3142.
13. G. Liu, R. Lan, P. Mu, Y. Shen and B. Zhao, *Opt. Commun.*, 2022, **523**, 128737.
14. B. Fu, P. Wang, Y. Li, M. Condorelli, E. Fazio, J. Sun, L. Xu, V. Scardaci and G. Compagnini, *Nanophotonics*, 2020, **9**, 3873-3880.
15. T. Wang, J. Wu, H. Wu, J. Wang, L. Huang and P. Zhou, *Opt. Laser Technol.*, 2019, **119**, 105618.
16. Y.-J. Sun, C.-K. Lee, J.-L. Xu, Z.-J. Zhu, Y.-Q. Wang, S.-F. Gao, H.-P. Xia, Z.-Y. You and C.-Y. Tu, *Photonics Res.*, 2015, **3**, A97.
17. M. Liu, D. Zhou, Z. Jia, Z. Li, N. Li, S. Li, Z. Kang, J. Yi, C. Zhao, G. Qin, H. Song and W. Qin, *J. Mater. Chem. C.*, 2017, **5**, 4034-4039.
18. X. Ma, C. Wang, J. Zhang, T. Wang, A. Wang, S. Wang, Z. Jia, B. Zhang, J. He, S. van Smaalen and X. Tao, *Adv. Opt. Mater.*, 2022, **10**, 2201087.
19. N. Li, H. Jia, M. Guo, W. Zhang, J. Wang and L. Song, *Nano Res.*, 2022, **15**, 4403-4410.
20. S. Ahmed, J. Qiao, P. K. Cheng, A. M. Saleque, M. N. A. S. Ivan, T. I. Alam and Y. H. Tsang, *ACS Appl. Mater. Interfaces.*, 2021, **13**, 61518-61527.